

Effect of carbon on hydrogen desorption and absorption of mechanically milled MgH_2

C.X. Shang, Z.X. Guo*

Department of Materials, Queen Mary University of London, Mile End Road, London E1 4NS, UK

Abstract

The use of MgH_2 , instead of pure Mg, in the mechanical synthesis of Mg-based hydrogen storage materials offers added benefit to powder size refinement and reduced oxygen contamination. Alloying additions can further improve the sorption kinetics at a relatively low temperature. This paper examines the effect of graphitic carbon on the desorption and absorption of MgH_2 . Graphite powder of different concentrations were mechanically milled with MgH_2 particles. The milled powder was characterised by XRD, SEM and simultaneous TG and DSC techniques. The results show that graphite poses little influence on the desorption properties of MgH_2 . However, it does benefit the absorption process, leading to rapid hydrogen uptake in the re-hydrogenated sample. After dehydrogenation, 5 wt.% of hydrogen was re-absorbed within 30 min at 250 °C for the ($\text{MgH}_2 + 10\text{G}$) mixture prior-milled for 8 h, while only 0.8 wt.% for the pure MgH_2 milled for 8 h, the effect may be attributed to the interaction between crystalline graphite with H_2 disassociation close to the MgH_2 or Mg surface. Moreover, graphite can also inhibit the formation of a new oxide layer on the surface of Mg particles.

© 2003 Elsevier B.V. All rights reserved.

Keywords: Mechanical milling; Magnesium hydride; Carbon

1. Introduction

Metal hydrides are of considerable interest for safe and practical hydrogen storage. Among these, MgH_2 is regarded as a very promising hydrogen storage material for vehicular applications, due to its high theoretical hydrogen-storage capacity of about 7.6 mol%, light weight and low cost. However, relatively high sorption temperatures and low kinetics are main obstacles hindering its commercial applications. Moreover, for the first hydrogen uptake, Mg usually needs to be “activated” by being exposed to a high temperature and a high hydrogen pressure for 10 h [1]. This is due to the fact that the surface oxide/hydroxide layer in Mg is impermeable to hydrogen. Therefore, the surface of Mg must always be clean to allow hydrogen to reach the underlying Mg.

Apart from metallic alloying [1], some non-metal elements have also been studied as additives to Mg to improve its hydrogen storage properties. For instance, graphite carbon has recently been noted to facilitate the activation process of Mg and improve the absorption kinetics of both Mg and Mg_2Ni [2–5]. Imamura et al. [4,5] have used organic additives, such as benzene and cyclohexane, in Mg/graphite mixtures to enhance the solid-phase interaction between

graphite and Mg during milling and to prevent the graphite from excessive breakage or becoming amorphous. Amorphous graphite does not seem to interact with Mg and the benefit to activation of H absorption cannot be realised either. The authors have also identified that the additives promote the transformation of graphite into thin flakes with cleavage planes normal to the surface of Mg and such a structure influences strongly the hydrogen storage properties of the mixture, e.g. rapid absorption kinetics can be achieved at 180 °C.

The use of MgH_2 , instead of pure Mg, as a starting material can offer several additional advantages during mechanical synthesis of hydrogen storage systems, such as much refined grain size and reduced oxygen contamination [6]. However, there has been no report regarding the effect of carbon on MgH_2 as a starting powder and on the hydrogen desorption properties of Mg or MgH_2 powder milled with carbon. Here, both of hydrogen desorption and absorption properties of the MgH_2 powder milled with graphite carbon, termed as the ($\text{MgH}_2 + \text{G}$) mixture, were investigated. The results were discussed along with earlier findings on pure Mg.

2. Experimental methods

MgH_2 powder was purchased from Th. Goldschmidt AG, with a nominal composition of 95 mol% MgH_2 and 5 mol% Mg and an average diameter of 50 μm . Crystalline

* Corresponding author. Tel.: +44-20-78825569;

fax: +44-20-89819804.

E-mail address: x.guo@qmul.ac.uk (Z.X. Guo).

graphite powder (99 mass%, 45 μm) was purchased from Goodfellow. A Fritsch P5 planetary ball mill with sealed pots was used for mechanical milling under an inert argon atmosphere. The elements were weighted in a glove box filled with high purity argon. Each experiment involved about 6 g of powder and six stainless-steel balls of 20 mm in diameter, leading to a ball-to-powder weight ratio of 30. A relatively low milling speed of 168.4 rpm was chosen in the study.

For hydrogen desorption examination, three compositions of graphitic carbon 1, 10 and 30 mol% were first mixed with MgH_2 for 1 h to identify the actual effect of different graphite contents on the dehydrogenation of MgH_2 and then the sample with 10 mol% of graphite was further milled with MgH_2 for 4, 8 and 15 h to investigate the milling effect on the structural stability and hydrogen desorption of the mixture, which is termed as $(\text{MgH}_2 + 10\text{G})$.

In order to identify the possible effect of carbon on hydrogen absorption, the $(\text{MgH}_2 + 10\text{G})$ mixtures milled for 1, 4 and 8 h were first dehydrogenated at 430 $^\circ\text{C}$ for 2 h under vacuum to ensure complete release of hydrogen, guided by prior study of hydrogen desorption of MgH_2 [7] and then rehydrogenated at a relatively low temperature of 250 $^\circ\text{C}$ for 30 m under 12–14 bar of hydrogen pressure for one cycle; the temperature was chosen deliberately to a very low value in order to enhance the difference in hydrogenation with and without graphite. The absorption half-cycle was not closely followed in this experiment due to lack of an accurate monitoring system. Instead, the desorption of the rehydrogenated samples were studied using simultaneous thermogravimetry (TG) and diffraction scanning calorimetry (DSC) to identify the total hydrogen absorbed under the preset rehydrogenation conditions.

To further clarify whether additional powder boundaries may enhance hydrogen “storage”, a loose and a compacted $(\text{MgH}_2 + 10\text{G})$ mixtures prior-milled for 8 h were first dehydrogenated at 430 $^\circ\text{C}$ for 2 h, and then rehydrogenated at 350 $^\circ\text{C}$ for 6 h under 14 bar hydrogen pressure. The compacted pellet sample was made in a die using about 0.065 g of the milled powder and a 15 ton cold press. During each compaction, a pressure of 220 bar was used to make a thin pellet with a diameter of 6 mm and a thickness of about 0.5–0.6 mm. Structural and hydrogen desorption/absorption characterisations of the samples were performed by X-ray diffraction (XRD), scanning electron microscopy (SEM) as well as simultaneous TG/DSC.

3. Results

3.1. Structural characterisations by XRD and SEM

The phase evolution of the $(\text{MgH}_2 + 10\text{G})$ mixture with milling time was examined by XRD analyses and the results are shown in Fig. 1. The peak at $2\theta = 26^\circ$ belongs to the crystalline graphite. Its intensity is reduced gradually with the increase of milling time. After 15 h of milling, no

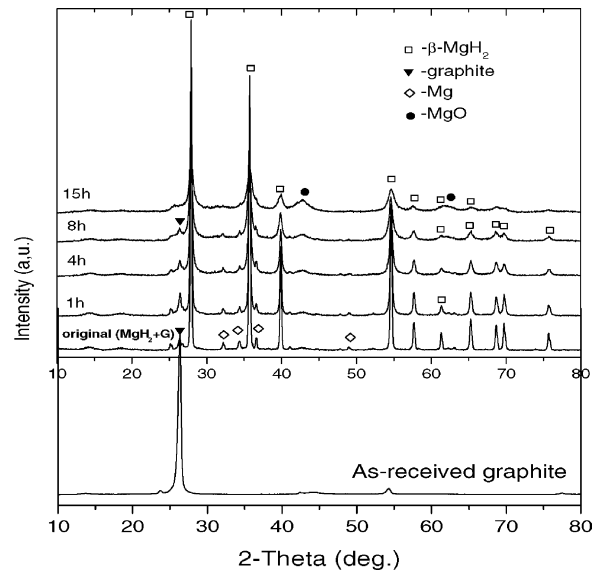


Fig. 1. Evolution of XRD patterns of the $(\text{MgH}_2 + 10\text{G})$ mixture with milling time.

graphite peaks were detected, which indicates that the regular crystalline structure of the graphite has been destroyed by milling, leading to undesirable amorphization. In order to maintain the crystalline structure of graphite, it is suggested that milling should be less than 15 h under the current conditions. Some MgO was produced during milling due to the easy oxidation of residual Mg remaining in the parent MgH_2 .

The as-received MgH_2 powder was also milled for 8 and 15 h for comparison with the $(\text{MgH}_2 + 10\text{G})$ mixture. The XRD patterns of the milled powder/mixture were shown in Fig. 2. It is noted that the intensity and width of the MgH_2 peaks for the $(\text{MgH}_2 + 10\text{G})$ mixture are similar to those for the MgH_2 milled for the same period of time, indicating

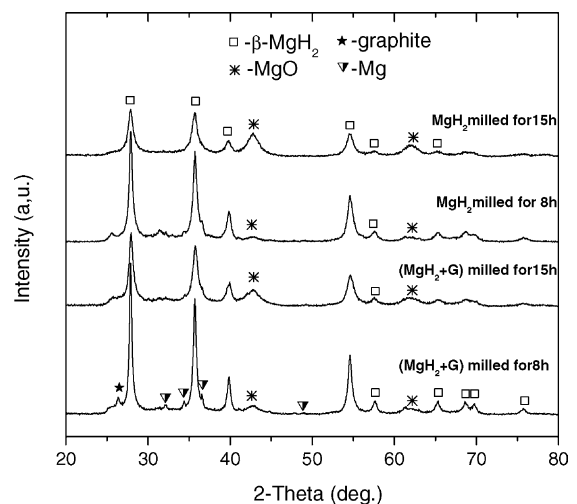


Fig. 2. Comparison of XRD patterns of the pure MgH_2 and the $(\text{MgH}_2 + 10\text{G})$ mixture milled for 8–15 h under the same milling conditions.

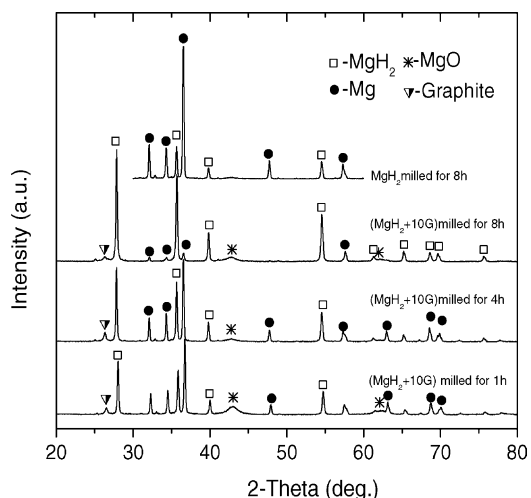


Fig. 3. XRD patterns of the milled MgH_2 and $(\text{MgH}_2 + 10\text{G})$ mixtures rehydrogenated at 250°C for 30 min after dehydrogenation at 430°C for 2 h.

that the crystallite size of the $(\text{MgH}_2 + 10\text{G})$ mixture was not affected by the addition of graphite during milling and is similar to that of the MgH_2 .

The milled mixtures were completely dehydrogenated and then rehydrogenated at 250°C for 30 min. Fig. 3 illustrates the XRD patterns of the rehydrogenated $(\text{MgH}_2 + 10\text{G})$ mixtures originally milled for 1, 4 and 8 h, along with a rehydrogenated MgH_2 sample originally milled for 8 h. It is seen that the intensities of the pure MgH_2 peaks are greater and those of pure Mg are weaker for the rehydrogenated mixture prior-milled for a longer period of time, which means that more hydrogen was absorbed in the mixture. By comparison with the XRD pattern of the pure MgH_2 prior-milled

for 8 h after rehydrogenation under the same conditions, it is clearly noted that the MgH_2 peaks of the $(\text{MgH}_2 + 10\text{G})$ mixture are much higher than those of the pure MgH_2 , while the Mg peaks of the mixture are much lower than those of pure MgH_2 . This observation indicates that a greater amount of the hydride has been formed in the $(\text{MgH}_2 + 10\text{G})$ mixture than in the pure MgH_2 after rehydrogenation. Moreover, it should be noted that crystalline graphite exists in all the rehydrogenated mixtures, implying that the graphite did not react or did not react strongly with Mg or H_2 during cycling.

Fig. 4a–e compares the SEM images of the $(\text{MgH}_2 + 10\text{G})$ powder mixtures milled for 1, 4 and 8 h, the as-received graphite and the pure MgH_2 milled for 8 h, respectively. Clearly, the particle sizes are very different. The $(\text{MgH}_2 + 10\text{G})$ mixture milled for 1 h exhibits inhomogeneous particle size distribution. Many large particles are dispersed among small ones. With the increase of milling time, the particle size decreases and the particles gradually become homogeneous. Particularly, the mixture milled for 8 h shows very fine distribution Fig. 4c).

Also from Fig. 4c–e, it is clearly noted that after milling, there is a significant size reduction of the graphite particles and moreover, the particle size of the $(\text{MgH}_2 + 10\text{G})$ mixture milled for 8 h is smaller and also more uniform than that of the pure MgH_2 milled for 8 h.

In order to see whether rehydrogenation alters the particle size of the cold pressed pellet, it was cut in half, mounted in resin and polished slightly for easy examination. The SEM images of the pellet specimen of the $(\text{MgH}_2 + 10\text{G})$ mixture prior-milled for 8 h are compared in Fig. 5 after dehydrogenation at 430°C for 2 h and Fig. 6 after rehydrogenation at 350°C for 6 h. At a low magnification,

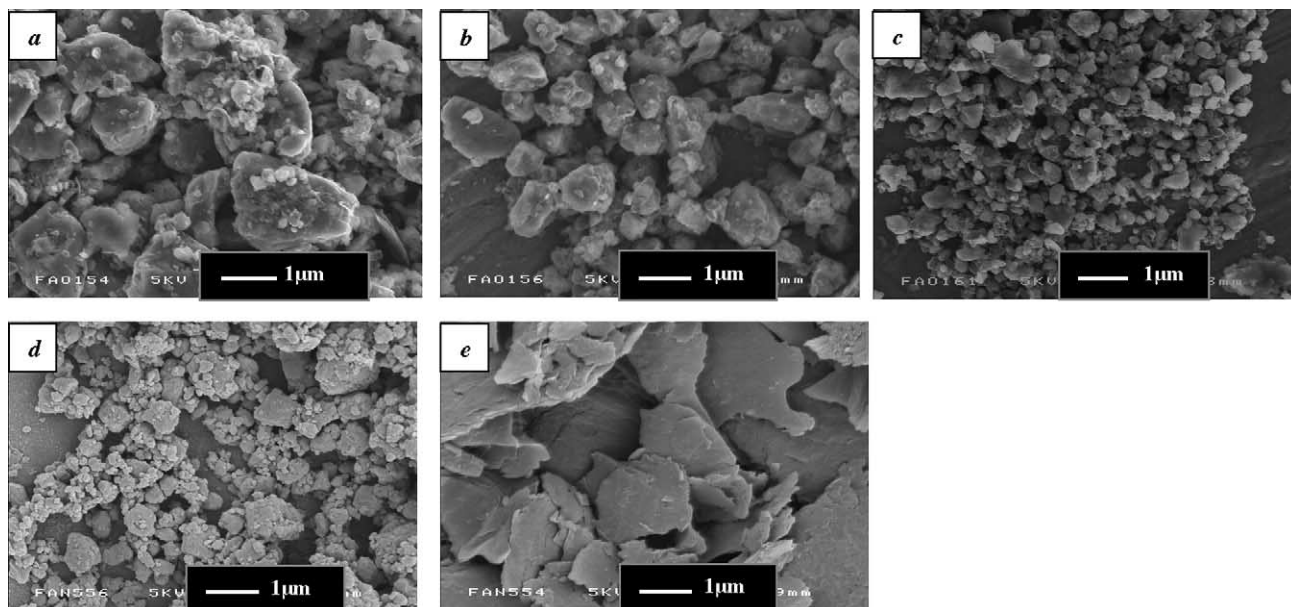


Fig. 4. SEM images of the $(\text{MgH}_2 + 10\text{G})$ powder mixture milled for: (a) 1 h, (b) 4 h, (c) 8 h and (d) of MgH_2 milled for 8 h and (e) of the as-received graphite (micron bar = $1\ \mu\text{m}$).

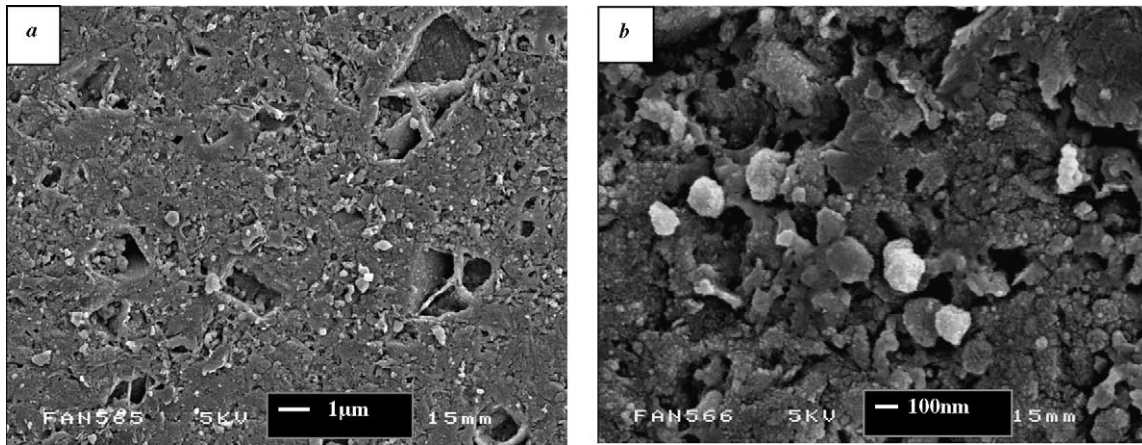


Fig. 5. SEM images of the $(\text{MgH}_2 + 10\text{G})$ mixture pellet originally milled for 8 h after dehydrogenation at 430°C for 2 h: (a) at a low magnification and (b) at a high magnification.

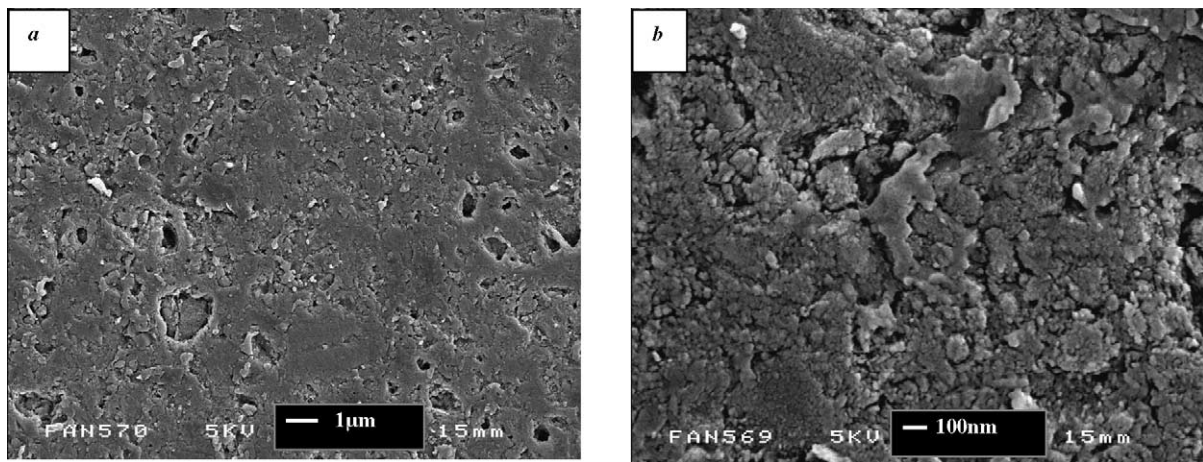


Fig. 6. SEM images of the $(\text{MgH}_2 + 10\text{G})$ pellet originally milled for 8 h after rehydrogenation at 350°C for 6 h: (a) at a low magnification and (b) at a high magnification.

Figs. 5(a) and 6(a)), there seems not much difference between the two samples, apart from the evidence of a porous structure in both cases, which may be useful in trapping hydrogen inside the material. No additional cracking of the samples is seen, which indicates that the cold compacted sample is able to stand hydrogenation/dehydrogenation cycling. At the higher magnification, Figs. 5(b) and 6(b)), the particles seem more uniform after rehydrogenation, possibly due to that the newly formed hydrides break up relatively large agglomerates in the sample during rehydrogenation.

3.2. Hydrogen desorption properties of the milled $(\text{MgH}_2 + \text{G})$ mixtures

Fig. 7 shows the DSC traces of the mixtures of MgH_2 milled with 1, 10 and 30 mol% of graphite for 1 h at a low speed of 168 rpm (dial number 4). The hydrogen desorption peaks only defer by a few degrees with the increase of carbon content, the onset desorption temperature was not reduced, all starting at about 400°C . Therefore, the content of

graphite in MgH_2 does not seem to influence the hydrogen desorption temperature of the mixture.

The $(\text{MgH}_2 + 10\text{G})$ mixture was selected for further milling up to 4, 8 and 15 h, respectively. The DSC traces of the mixtures after different periods of milling are compared in Fig. 8. There is a slight reduction in the desorption peak as milling time increases, which may be attributed to

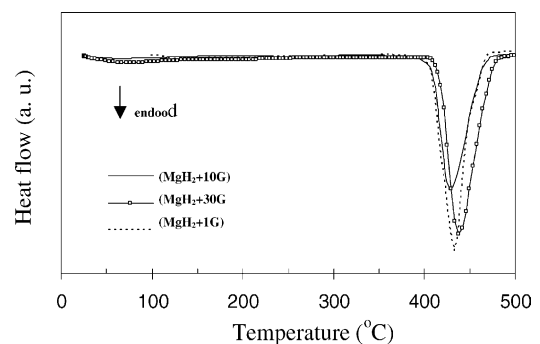


Fig. 7. DSC traces of the mixtures of $(\text{MgH}_2 + 1, 10$ and 30 mol\% graphite) milled for 1 h at a low speed of 168 rpm.

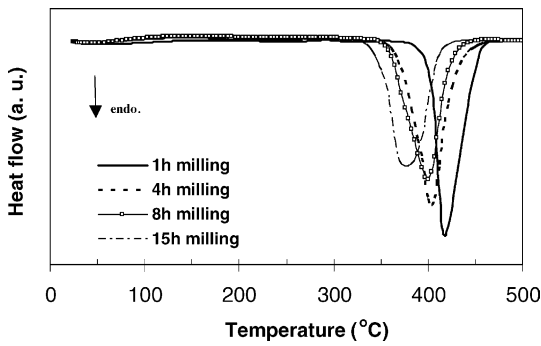


Fig. 8. DSC traces of dehydrogenation of the (MgH₂ + 10G) mixture initially milled for different periods of time.

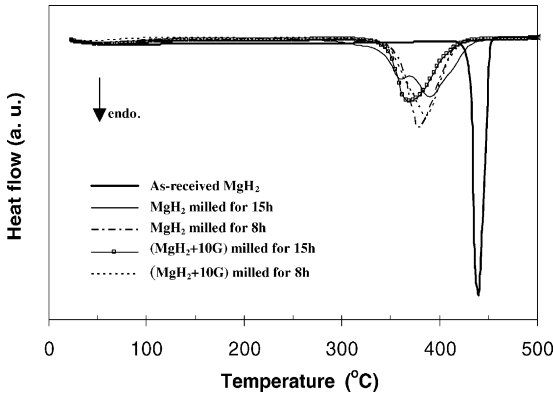


Fig. 9. Comparison of DSC traces of dehydrogenation of the MgH₂ and the (MgH₂ + 10G) mixtures initially milled for 8 and 15h, respectively.

particle size reduction due to milling. To clarify this point, the curves are further compared with those of the pure MgH₂ milled for 8 and 15 h in Fig. 9. The peak positions of the pure MgH₂ and the (MgH₂ + 10G) milled for the same length of time are more or less the same, which indicates that graphite has little effect on the desorption temperature. Therefore, the peak shifts shown in Fig. 8 are mainly the result of powder size reduction.

Figs. 4–10 show the mass loss as a function of temperature, simultaneously measured with the DSC curves given

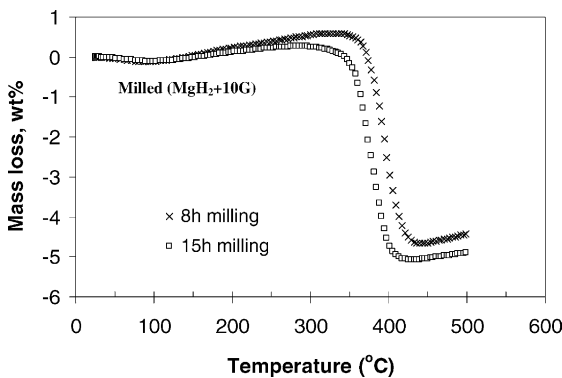


Fig. 10. Weight loss of hydrogen desorption of the prior-milled (MgH₂ + 10G) mixture as a function of temperature, simultaneously measured with the DSC measurements in Fig. 8.

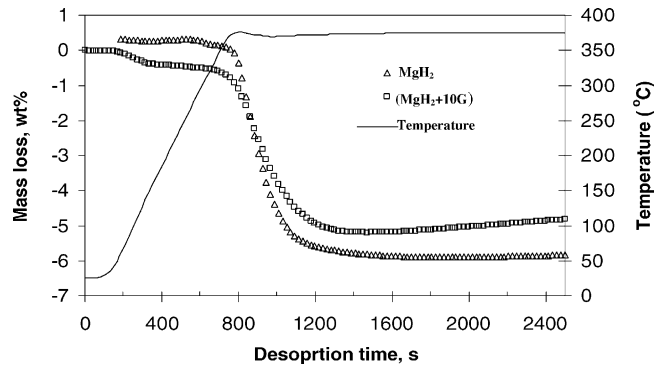


Fig. 11. Comparison of hydrogen desorption kinetic curves at 375 °C, of the prior-milled MgH₂ and (MgH₂ + 10G) mixture for 8h.

in Fig. 8, for two (MgH₂ + 10G) samples milled for 8 and 15 h, respectively. It reveals the total amount of hydrogen that can be released from the milled mixtures, which is about 5 wt.% in both cases. Since the DSC curves in Fig. 8 indicate that the on-set desorption temperature is around 370 °C, isothermal TG tests were carried out at 375 °C for MgH₂ and the (MgH₂ + 10G) mixture milled for 8 h. The results are illustrated in Fig. 11, where the desorption kinetics are noted to be similar. This further confirms that graphite has little effect on the hydrogen desorption properties of MgH₂.

3.3. Hydrogen desorption of the rehydrogenated (MgH₂ + G) mixtures

Fig. 12 shows the DSC traces of the rehydrogenated (MgH₂ + 5G) mixture originally milled for 1, 4 and 8 h, respectively (the sample milled for 15 h was not selected because the carbon structure was largely destroyed, as indicated in Fig. 1). The endothermic desorption peaks of the rehydrogenated (MgH₂ + 5G) mixtures are in similar positions to those of their original counterparts, shown in Fig. 8, indicating that the rehydrogenation has not changed the onset desorption temperature.

The corresponding TG curves of the rehydrogenated (MgH₂ + 5G) mixtures are shown in Fig. 13, where the

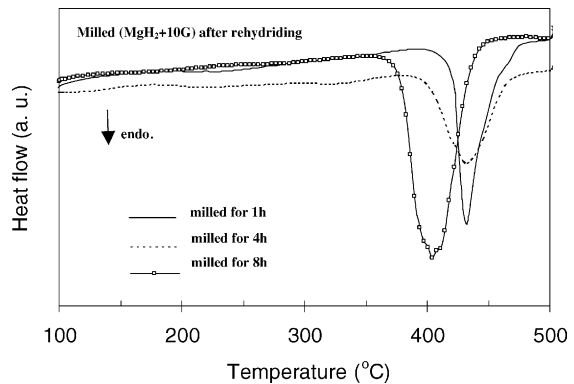


Fig. 12. DSC traces of the rehydrogenated (MgH₂ + 10G) mixture prior-milled for 1, 4 and 8h, respectively.

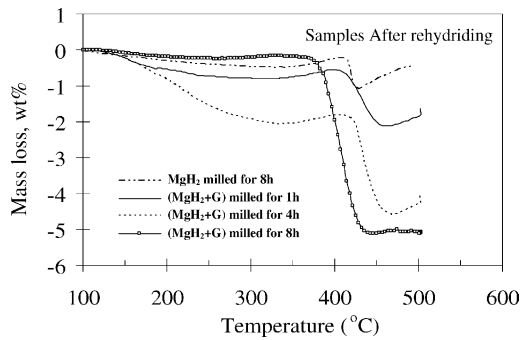


Fig. 13. TG curves of hydrogen desorption as a function of temperature of the rehydrided ($\text{MgH}_2 + 10\text{G}$) mixture prior-milled for 1, 4 and 8 h and the rehydrided MgH_2 prior-milled for 8 h.

hydrogen desorption capacities are 1.6, 2.8 and 5.0 wt.%, respectively, for the mixtures originally milled for 1, 4 and 8 h. The desorption curve of a pure MgH_2 milled for 8 h is also shown for comparison, where the sample is noted to have absorbed only about 0.8 wt.% hydrogen. This clearly demonstrates that carbon indeed facilitates the hydrogen absorption (here, the rehydrogenation) of the ($\text{MgH}_2 + 10\text{G}$) mixtures. The increased hydrogen up-take, indicated by the higher desorbed value, with increasing milling time is likely due to increased uniformity of carbon distribution on MgH_2 particle surfaces and a reduction in the particle size. Hence, the beneficial effects of elemental carbon on hydrogen absorption have been clearly identified.

Fig. 14 compares the DSC and TG curves of the loose powder and the pellet of the rehydrogenated ($\text{MgH}_2 + 10\text{G}$) mixture originally milled for 8 h. Both TG and DSC curves show that the hydrogen desorption temperatures and kinetics of the powder and the pellet are very similar. The TG curves show that hydrogen released from the powder and the pellet is about 5.0 and 6.0 wt.%, respectively. The small enhancement in the hydrogenation capacity in the pellet may be due to closely packed powder interfaces or boundaries, which provide additional sites for storing hydrogen.

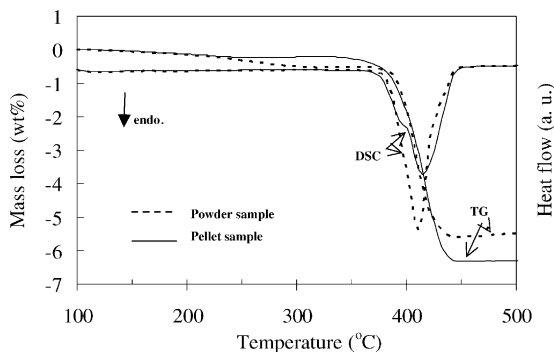


Fig. 14. Comparison of the DSC and TG curves of the powder sample and the pellet sample of the rehydrogenated ($\text{MgH}_2 + 10\text{G}$) mixture (8 h milling) at 350 °C for 6 h under 14 bar H_2 pressure.

4. Discussion

To reduce the time needed for full activation and fast H uptake of Mg, it has been noted that crystalline carbon improves the activation behaviour and absorption kinetics of Mg or Mg_2Ni . Milling Mg with as little as 10 wt.% of graphite for only 30 min has been shown to generate much more rapid H uptake at 300 °C than pure Mg milled for a longer period of time under the same milling conditions [2,3]. The material can be fully activated by the addition of graphite, which inhibits the formation of a new oxide layer once the initial oxide layer is broken.

In the relatively less energetic milling condition (speed: 168.4 rpm), the phase evolution of the ($\text{MgH}_2 + 10\text{G}$) with milling time was shown in Fig. 1. It took about 15 h of milling to destroy completely the crystalline structure of graphite, as indicated by the disappearance of the characteristic diffraction peaks of graphite. As report by Imamura et al. destroyed graphite structure does not influence the surface and interface state of the material, Therefore, the milling should be limited to a short period of time, no more than 15 h in order to present the effect of graphite on absorption of hydrogen. The position of the diffraction peaks of MgH_2 shows no shift with milling, indicating that the dissolution of C into MgH_2 did not occur, at least not to a significant extent. This is in agreement with the report in the binary phase diagram that the solubility of C in Mg is extremely low [8].

By comparison of the XRD patterns of the MgH_2 milled for 8–15 h with those of the ($\text{MgH}_2 + 10\text{G}$) milled for the same periods of time Fig. 2, the addition of graphite does not significantly change the crystallite size of MgH_2 . This is different from the result by [3], in which a sizeable reduction of the crystalline size of Mg is reported, even after milling Mg with graphite for only 30 min. The difference is possibly due to that the MgH_2 is very brittle and its crystallite size is already very small in our case. However, Bouaricha et al. also show that the reduction of the crystallite size is not responsible for the improved activation characteristics of the material.

Moreover, the SEM images in Fig. 4 show that the ($\text{MgH}_2 + 10\text{G}$) mixture milled for 8 h consists of more uniform and smaller particles than the MgH_2 milled for the same period of time. This may be partly due to that the addition of graphite reduces the adhesion and agglomeration of MgH_2 particles. These fine particles have large surface area per unit volume, which can enhance the hydrogen diffusion and hydride phase formation, therefore, of benefit to the sorption kinetics. Bouaricha et al. [2] have also reported that various C-containing materials such as fullerene and graphite can increase the specific surface area of nanocrystalline Mg_2Ni . However, these carbon additions show no effect on the hydrogen desorption kinetics of Mg_2Ni .

Graphite does not seem to react with other elements during dehydrogenation and hydrogenation. This has been proved in Fig. 3 for the XRD patterns of the ($\text{MgH}_2 + 10\text{G}$) mixture rehydrogenated at 250 °C after dehydrogenation,

where the graphite still remains in the mixture among the Mg/MgH₂ particle. Therefore, the changes in hydrogen absorption/desorption properties of the mixture should be related to the addition of graphite. The observation agrees with the finding in [3,5].

For the milled (MgH₂ + G) mixtures with different graphite contents, the desorption temperature stays more or less the same, Fig. 7. Although further milling of the (MgH₂ + G) mixture up to 15 h leads to about 70 °C reduction in the desorption temperature, Figs. 8 and 9, compared with the as-received MgH₂. Such a reduction is mainly due to the milling effect as a result of reduced particle size. Hence it can be firmly stated that the addition of graphite in MgH₂ does not influence the desorption temperature. Neither does graphite seem to influence the desorption kinetics as seen in Fig. 11. Graphite in the samples does not interact with or catalyse the MgH₂ particles.

The existing experimental facility prohibits direct measurements of the absorption kinetic curves. In order to clarify whether the graphite influences the absorption behaviour of MgH₂, the milled (MgH₂ + G) mixture was first dehydrogenated completely then rehydrogenated and finally the “absorption” characteristics of the mixtures are inferred from the desorption curves of the rehydrogenated samples. This is particularly noted in Fig. 13, where the total amount of hydrogen released in the samples corresponds to the total amount of hydrogen absorbed during the rehydrogenation process. Clearly, there is more hydrogen absorbed in the graphite modified mixtures than in the simply milled MgH₂. The higher level of hydrogen absorbed in the mixture milled for a longer period of time may be due to a more uniform coverage of carbon around even smaller particles, both of which facilitate rapid hydrogen uptake in the sample. This point is also clearly illustrated in the relative intensities of the diffraction peaks, shown in Fig. 3. The MgH₂ peaks in the graphite modified samples are much higher than those in the pure MgH₂. This cannot be solely attributed to the milling effect as result of particle size reduction, because the pure MgH₂ was milled for 8 h as well, but did not show much absorbed hydrogen. Therefore, the crystalline graphite should play a certain catalytic role in the hydrogen absorption of Mg, or dissociation of H₂ near the Mg surface.

Moreover, Fig. 3 also indicates that a lower level of MgO exist in the mixture prior-milled for a longer period of time (4 and 8 h), which may also be related to more uniform distribution of graphite in the powder mixtures; uniformly distributed graphite forms an effective physical and/or reducing barrier to oxidation, and hence facilitate rapid hydrogenation, as observed in Fig. 13. Moreover, the desorption temperatures of the rehydrogenated mixtures are similar to those of the previously milled samples, Figs. 8 and 12; a slight shift to a higher temperature in the rehydrogenated samples prior-milled for 1 and 4 h (Fig. 12) may be due to a relatively high MgO level, see in Fig. 3, and/or some level of preferred particle growth in these samples, where the graphite is not as uniformly distributed as in the 8 h-milled sample.

Attempt to identify whether a firmly compacted powder pellet can store more hydrogen than a loosely compacted powder sample that was made using the (MgH₂ + 10 mol% G) mixture. The results indeed confirm a small increase in the hydrogen absorption capacity of the pellet by about 1 wt.%, Fig. 14, because of additional powder–particle boundaries and/or small pores that can trap hydrogen in the sample. Hence, the smaller the particle size, the greater this “compacting” effect is likely to be. Nano-sized powder mixtures may gain the maximum benefit from much enhanced powder boundaries.

As with other alloying additions to improve the sorption temperature and kinetics, increasing the level of carbon is likely to reduce the overall hydrogen storage capacity, unless the carbon structure happens to absorb/desorb hydrogen readily as well. When the “mist” on hydrogen storage of carbon nanostructures is clear, it is possible to identify an optimum hydrogen-absorbing carbon nanostructure as an ideal modifier to Mg surfaces for the benefit of improving both the sorption properties and the storage capacity.

5. Conclusions

The possible effects of crystalline graphite on the hydrogen desorption and absorption characteristics of MgH₂ were investigated in this article. The results clearly show that graphite poses little influence on desorption temperature and kinetics of MgH₂. However, it does benefit the absorption behaviour of MgH₂, leading to rapid hydrogen uptake in the rehydrogenated sample. After dehydrogenation, 5 wt.% of hydrogen was re-absorbed within 30 min at 250 °C for the (MgH₂ + 10 G) mixture prior-milled for 8 h, while only 0.8 wt.% for the pure MgH₂ milled for 8 h, the effect may be attributed to the interaction between crystalline graphite and the disassociation of hydrogen molecules at the MgH₂ or Mg surface and graphite coating on the powder particles can also inhibit the formation of a new oxide layer on the Mg powder surfaces.

Acknowledgements

This project was supported by the EPSRC (Grant No. GR/R82074/01). Helpful discussions with Dr. S. Dodd, QinetiQ and Dr. B. Lakeman, DSTL, are gratefully acknowledged.

References

- [1] C.X. Shang, M. Bououdina, Y. Song, Z.X. Guo, *Int. J. Hydrogen Energy*, in press.
- [2] S. Bouaricha, J.P. Dodelet, D. Guay, J. Huot, S. Boily, R. Schulz, *J. Alloys Comp.* 307 (2000) 226.
- [3] S. Bouaricha, J.P. Dodelet, D. Guay, J. Huot, R. Schulz, *J. Alloys Comp.* 325 (2001) 245.

- [4] H. Imamura, S. Tabata, N. Shigetomi, Y. Takesue, Y. Sakata, *J. Alloys Comp.* 330–332 (2002) 579.
- [5] H. Imamura, S. Tabata, Y. Takesue, Y. Sakata, S. Kamazaki, *Int. J. Hydrogen Ener.* 25 (2000) 837.
- [6] C.X. Shang, M. Bououdina, Z.X. Guo, *J. Alloys Comp.* 349 (2003) 217.
- [7] J. Huot, G. Liang, S. Boily, A. Van Neste, R. Schulz, *J. Alloys Comp.* 293–295 (1999) 495.
- [8] A. A. Nayeb-Hashemi, J. B. Clark (Eds.), *Phase Diagrams of Binary Magnesium Alloys*, ASM International, Metals Park, OH, 1988.